

Base- and Additive-Free Carbon Dioxide Hydroboration to Methoxyboranes Catalyzed by Non-Pincer-Type Mn(I) Complexes

Sylwia Kostera, Stefan Weber, Ines Blaha, Maurizio Peruzzini, Karl Kirchner,* and Luca Gonsalvi*



Cite This: *ACS Catal.* 2023, 13, 5236–5244



Read Online

ACCESS |



Metrics & More



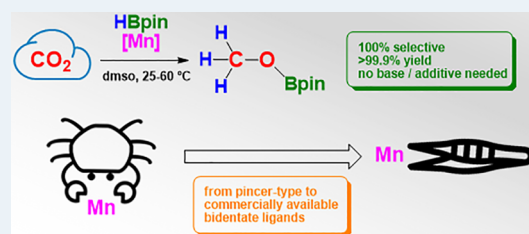
Article Recommendations



Supporting Information

ABSTRACT: Well-defined, bench stable Mn(I) non-pincer-type complexes were tested as earth-abundant transition metal catalysts for the selective reduction of CO₂ to boryl-protected MeOH in the presence of pinacolborane (HBpin). Essentially, quantitative yields were obtained under mild reaction conditions (1 bar CO₂, 60 °C), without the need of any base or additives, in the presence of the alkylcarbonyl Mn(I) bis(phosphine) complexes *fac*-[Mn(CH₂CH₂CH₃)(dippe)(CO)₃] [**Mn1**, dippe = 1,2-bis-(diisopropylphosphino)ethane] and [Mn(dippe)(CO)₂{(μ-H)₂(Bpin)}] (**Mn4**), that is obtained by reaction of the bench-stable precatalyst **Mn1** with HBpin via elimination of butanal. Preliminary mechanistic details were obtained by a combination of NMR experiments and monitoring of the catalytic reactions.

KEYWORDS: carbon dioxide utilization, manganese, organometallics, catalytic hydroboration, methanol



Carbon dioxide (CO₂) represents one of the principal greenhouse gases that are causing environmental concern for their increasing concentration in the atmosphere due to the growing consumption of fossil fuels. In spite of that, the unique characteristics of CO₂ as an inexpensive, nontoxic, and nonflammable chemical, together with its abundance as raw material, make it attractive for chemists interested in the synthesis of C1-products from renewable sources.¹ Chemical utilization of CO₂ is indeed growing in interest, and an increasing amount of literature describing transition metal or metal-free catalytic processes to reduce CO₂ to useful bulk chemicals such as formic acid (HCOOH) and methanol (CH₃OH) have been reported, especially in the last two decades.²

CH₃OH, currently produced in about 98 Mt/year quantity worldwide from fossil-based, nonrenewable feedstock under harsh conditions, is a valuable chemical product finding various large-scale direct application.³ In the pharmaceutical industry, it is employed as a starting compound for the production of various intermediates. It is also used to obtain formalin, i.e., a saturated aqueous solution of formaldehyde, which has strong bactericidal properties. It is an important solvent in organic synthesis, as a fuel or fuel component in internal combustion engines and as an additive to gasoline to improve the octane number, in household chemicals as a component of washing liquids and antifreeze, and in construction chemicals for the production of adhesives, paints, and varnishes. It is also an antibacterial, bactericidal, and fungicidal substance and utilized in the production of cosmetics and as a contaminant in some goods to deter consumption and inhalation.⁴ Due to its importance, the synthesis of CH₃OH from renewable feedstock such as CO₂ would be highly desirable, but efficient

catalysts must be designed to decrease the energy demand for the activation of such an inert small molecule by a 6-electron reduction process. Reduction of CO₂ to methanol or methoxy derivatives can be carried out under homogeneous catalytic conditions in the presence of non-noble⁵ and noble metals complexes⁶ and organocatalysts.⁷

In CO₂ reduction protocols, hydrogen (H₂) gas is generally preferred, in particular when it is obtained from sustainable, fossil-free sources and processes (i.e., water electrolysis, water photosplitting). However, the use of a pressurized, explosive gas such as H₂ has safety drawbacks and high costs of production, storage, and transportation. Alternative reducing agents for CO₂ such as hydroboranes can be promising to replace H₂ in the presence of highly active and selective catalysts that bring about the process under atmospheric pressure and mild temperature conditions.^{4–7} Boron-based compounds are generally Lewis acidic and oxophilic enough to enable activation of the C=O bond of carbon dioxide. Reduction of CO₂ by a hydroborane (Scheme 1) can lead to a variety of products such as formoxyborane (A), bis(boryl)-acetal (B), methoxyborane (C), and bis(boryl)ether (D).⁸ Therefore, high process selectivity is desired to achieve good atom-efficiency and to avoid distillation to separate the products present in the reaction mixtures.

Received: January 3, 2023

Revised: March 10, 2023

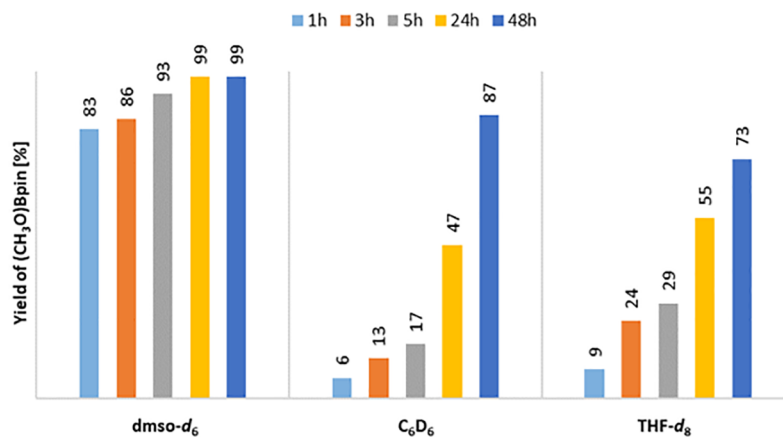


Figure 1. Solvent effect for CO₂ hydroboration to (CH₃O)Bpin in the presence of **Mn1**. Values correspond to yields of (CH₃O)Bpin (mol %). Reaction conditions are detailed in Table S1.

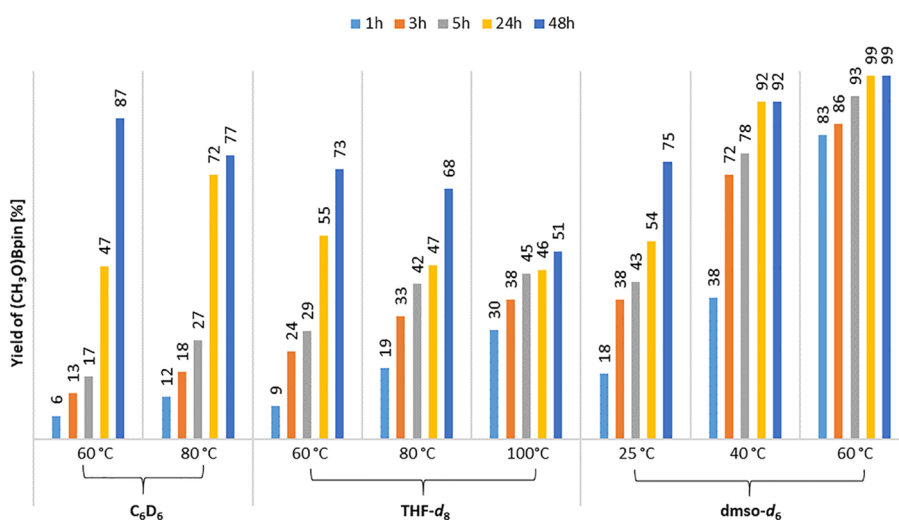


Figure 2. Temperature effect for CO₂ hydroboration to (CH₃O)Bpin in the presence of **Mn1**. Values correspond to yields of (CH₃O)Bpin (mol %). Reaction conditions are detailed in Table S2.

some of these systems gave high yields in the desired product without the need of base or additives, working under mild reaction conditions.

RESULTS AND DISCUSSION

Catalytic Tests. The catalytic tests were carried out on NMR tube scale, using catalysts **Mn1–4** (Chart 2), CO₂ (1 bar), HBpin (0.224 mmol), mesitylene as internal standard (0.056 mmol), no base or additives, monitoring the increase of the yields of C1-products (OCHO)Bpin (**A**), generally observed in small amounts or traces, and (CH₃O)Bpin (**C**) as the main product (Scheme 1, R₂B = Bpin) over time by ¹H NMR spectroscopy (see Experimental Section). Additional ¹¹B and ³¹P{¹H} NMR spectra were collected to obtain more details on the nature of the products and the changes in the catalyst in the course of the reactions. In all tests, the presence of (Bpin)₂O (**D**) was observed by ¹¹B NMR at 22.4 ppm, as expected for stoichiometry reasons. On the other hand, the formation of (Bpin)OCH₂O(Bpin) (**B**) was never observed in the corresponding ¹H NMR spectra. The effects of solvent, temperature, and ligands were screened in separate sets of experiments, and the results are hereby described.

Initially, the activity of precatalyst **Mn1** (1.0 mol % with respect to HBpin) in solvents such as dmsO-d₆, THF-d₈, and C₆D₆ was studied under standard reaction conditions (60 °C, 1 bar CO₂, HBpin 0.224 mmol). Noteworthy, dimethyl sulfoxide (dmsO) was previously demonstrated to assist CO₂ activation in hydrogenation^{2d} and in hydrosilylation reactions.^{5d} Under these conditions and using dmsO-d₆ as solvent, the reaction gave (CH₃O)Bpin, identified by the characteristic ¹H NMR signal at 3.48 ppm and the ¹¹B NMR broad signal at 20.9 ppm, as the main C1-product in very high yield (83%) after 1 h, and it increased further after 24 h (99%). Formoxyborane was observed to form in small amounts (ca. 6%) at the beginning of the reaction. No additional increase in yield was observed after 48 h (see Figure 1). Under the same reaction conditions, by changing solvent from dmsO-d₆ to either THF-d₈ or C₆D₆, (CH₃O)Bpin formed in yields lower than 60% within 24 h. After 48 h, (CH₃O)Bpin yields reached 87% and 73% in THF-d₈ and C₆D₆, respectively. The results are summarized as column graphs in Figure 1. Reaction conditions and details can be found in Table S1.

The effect of temperature was then investigated using **Mn1** as catalyst in the three different solvents mentioned above (Figure 2 and Table S2). The best results were confirmed in

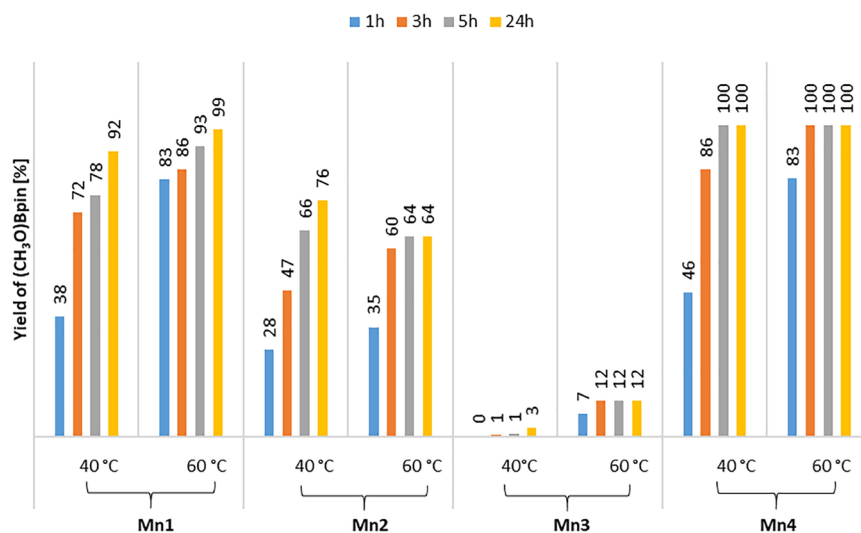


Figure 3. Ligand and temperature effects for CO₂ hydroboration to (CH₃O)Bpin in the presence of **Mn1**–**4**. Values correspond to yields of (CH₃O)Bpin (mol %). Reaction conditions are detailed in Table S3.

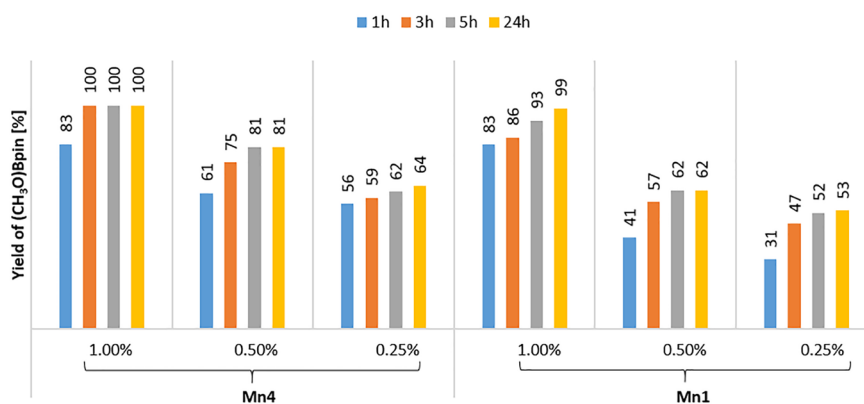


Figure 4. Catalyst amount screening in CO₂ hydroboration to (CH₃O)Bpin in the presence of **Mn4** and **Mn1**. Values correspond to yields of (CH₃O)Bpin (mol %). Reaction conditions are detailed in Table S4.

dms-*d*₆ at 60 °C with the formation of (CH₃O)Bpin in 83% (1 h) and 99% (24 h) yields. By decreasing the temperature to 40 °C, (CH₃O)Bpin was still obtained in high yield (92%) after 24 h. At room temperature, (CH₃O)Bpin formation reached 54% yield (24 h) and a remarkable 75% yield after 48 h. In C₆D₆ and THF-*d*₈, the lower performances already observed at 60 °C (Figure 1) were confirmed at 80 °C (max. yield 77% and 68%, 48 h, respectively) and at 100 °C in THF-*d*₈ (51%, 48 h).

Next, the effect of ligands was tested at 40 and 60 °C using **Mn1** analogues such as **Mn2**,¹⁶ **Mn3**,²⁰ and **Mn4**¹⁸ (Chart 2). The results are summarized in Figure 3 (see also Table S3). Compared to **Mn1**, in **Mn2**, the R substituents on P atoms were changed from ^{*i*}Pr to Cy, thus varying the steric hindrance of the complex. In **Mn3**, dippe was replaced by dppe [dppe = 1,2-bis(diphenylphosphino)ethane], and the alkyl ligand was changed from ^{*n*}Pr to CH₃. Finally, **Mn4** was obtained as previously shown¹⁸ from the reaction of **Mn1** with HBpin, giving a complex with a (μ-H)₂(Bpin) ligand that is more labile than ^{*n*}Pr under catalytic conditions.¹⁸ In other words, **Mn4** may represent an activated form of **Mn1** in hydroboration reactions.

Complex **Mn3** gave poor activity both at 40 and 60 °C with product **C** formation in only 3% and 12% yields after 24 h, respectively, thus confirming that under the conditions applied for CO₂ hydroboration, CH₃ is a worse leaving group than ^{*n*}Pr, as previously observed in other catalytic reactions.¹⁵ In the presence of **Mn2**, lower yields of product **C** were observed after 24 h compared to **Mn1**, both at 40 and 60 °C (76% and 64%, respectively). This is likely related to the higher solubility of **Mn1** than that of **Mn2** in dms-*d*₆. Interestingly, **Mn1** and **Mn4** showed a comparable behavior after 1 h of reaction, giving essentially the same yields of **C** at 60 °C. To our delight, almost quantitative yields of (CH₃O)Bpin were obtained in the presence of **Mn4** after only 3 h at 60 °C or after 5 h at 40 °C. Under the same conditions and time, **Mn1** gave instead 78% yield. Next, another test was run with **Mn4** as catalyst at 25 °C, reaching a yield of (CH₃O)Bpin of 52% after 5 h and 59% after 24 h.

Finally, the effect of catalyst amount was examined for **Mn1** and **Mn4**, using 0.25, 0.5, 1.0 mol % with respect to HBpin, running the tests in dms-*d*₆ at 60 °C for 24 h (Figure 4 and Table S4). At all chosen catalyst to substrate ratios, CO₂ hydroboration gave (CH₃O)Bpin as the main C1-product, with final yields varying in the range from 62 to >99%.

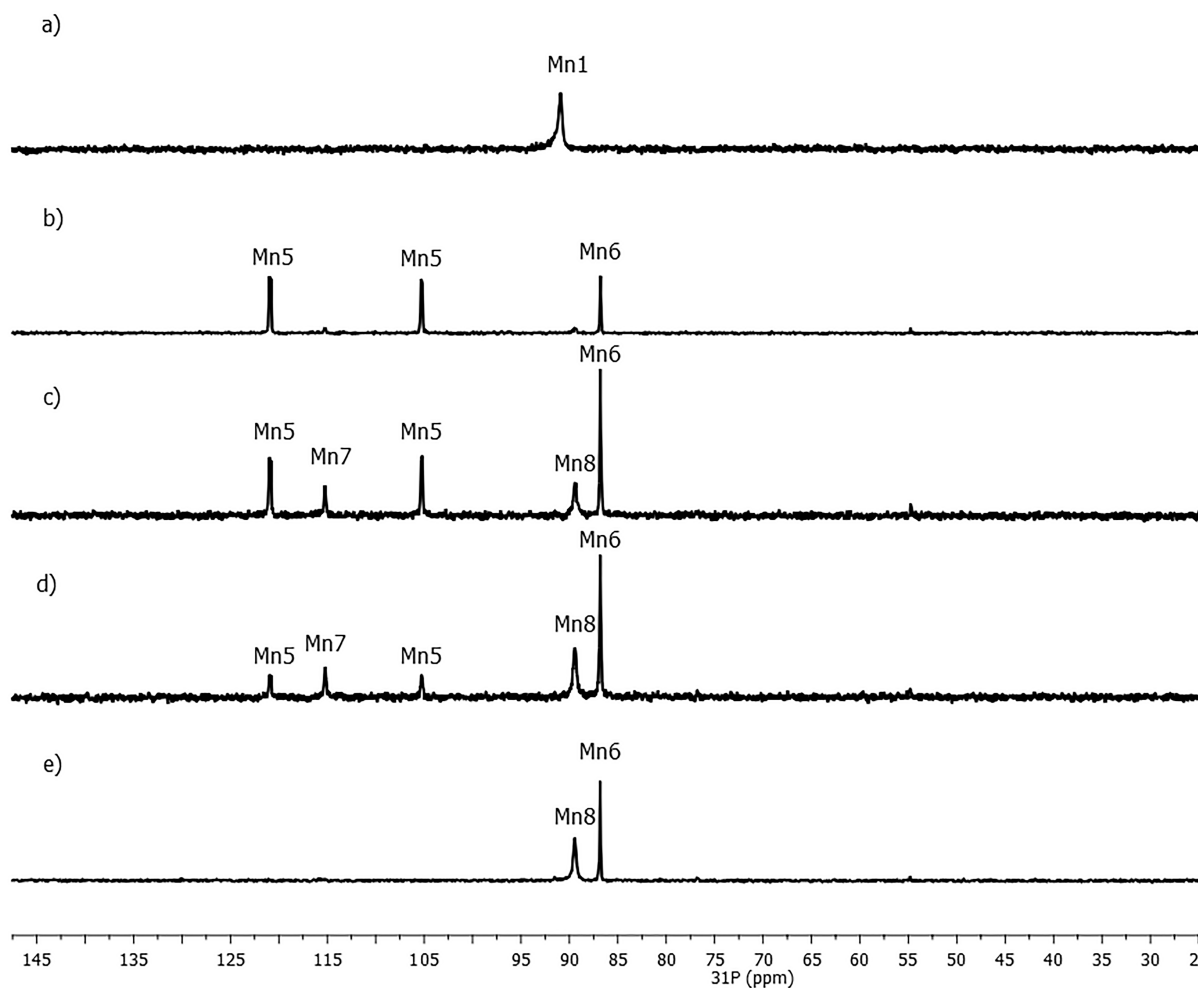


Figure 5. $^{31}\text{P}\{^1\text{H}\}$ NMR monitoring of a typical catalytic run. Reaction conditions: **Mn1** (2.24×10^{-3} mmol), HBpin (0.224 mmol), CO_2 (1 bar), 40°C , $\text{dms}\text{-}d_6$ (0.4 mL), mesitylene as internal standard (0.056 mmol). **Mn1** before (a) reaction and after (b) 1 h; (c) 3 h; (d) 5 h; (e) 24 h.

Although 1.0 mol % was confirmed as the most suitable catalyst amount to obtain the highest yields in $(\text{CH}_3\text{O})\text{Bpin}$, good results were also observed with 0.5 mol % in the case of **Mn4** (81% yield after 5 h). Catalyst deactivation may be responsible for the lower yields observed using 0.5 and 0.25 mol % of **Mn1** and **Mn4** (Figure 4). As recently highlighted in an excellent review article,²¹ a drop in yields may occur when the rate of catalyst deactivation competes with the catalytic rate, especially at high temperatures and at low catalyst concentrations.

A scaled-up (10-fold) Schlenk tube experiment, adapting the reaction conditions used for the highest yielding NMR test (i.e., **Mn1**, 60°C , 24 h, $\text{dms}\text{-}d_6$), was finally carried out. At the end of the reaction, $(\text{CH}_3\text{O})\text{Bpin}$ was obtained in >99.9% yield (see Experimental Section).

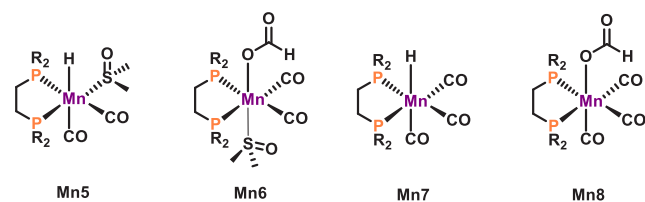
Mechanistic Studies. In order to get insights in the reaction mechanism, ^1H - and $^{31}\text{P}\{^1\text{H}\}$ NMR spectra were periodically recorded during the course of the catalytic reaction. The $^{31}\text{P}\{^1\text{H}\}$ NMR monitoring of the typical catalytic run in $\text{dms}\text{-}d_6$ is shown in Figure 5. After 1 h, **Mn1** was fully consumed, giving rise to the two new species **Mn5** and **Mn6**. After 3 h, signals due to the new species **Mn7** and **Mn8** were also detected along with **Mn5** and **Mn6**. After 24 h, **Mn6** and **Mn8** were the only species observable in the $^{31}\text{P}\{^1\text{H}\}$ NMR

spectrum. Essentially, the same results were achieved employing **Mn4** as precatalyst instead of **Mn1**.

In order to clarify the nature of the observed new species, additional NMR experiments were carried out. Complex **Mn5** was observed, further than during the catalytic run monitoring, also as the product of the reaction of **Mn1** with 5 equiv of HBpin in $\text{dms}\text{-}d_6$ at 40°C . It was then synthesized by the reaction of **Mn1** with HBpin (2 equiv) and $\text{dms}\text{-}d_6$ (2 equiv) in THF at 60°C (see Experimental Section). In the $^{31}\text{P}\{^1\text{H}\}$ NMR spectrum, **Mn5** is characterized by two doublets at 120.9 and 105.2 ppm, at the same chemical shift values observed during catalytic run monitoring, with a coupling constant $^2J_{\text{PP}} = 21.5$ Hz. In the corresponding ^1H NMR spectrum, a doublet of doublets was observed at -6.90 and -7.02 ppm, appearing as a pseudotriplet, with corresponding coupling constants $^2J_{\text{HP}} = 49.2$ Hz and $^2J_{\text{HP}} = 49.3$ Hz. Based on these data and on additional $^1\text{H}/^{31}\text{P}$ HMBC NMR spectra, we assign the structure of **Mn5** as *cis*- $[\text{MnH}(\text{dippe})(\text{CO})_2(\kappa\text{-S-dms})]$. **Mn5** could also be generated upon heating a solution of **Mn4** in $\text{dms}\text{-}d_6$ to 40°C . This behavior suggests that **Mn4** is likely to be an intermediate in the transformation from **Mn1** to **Mn5** in $\text{dms}\text{-}d_6$. An additional catalytic run under standard conditions (1.0 mol % to HBpin, 60°C , 24 h, $\text{dms}\text{-}d_6$) in the presence of **Mn5** as catalyst showed selective formation of $(\text{CH}_3\text{O})\text{Bpin}$ in >99.9% yield (Figure S.15). Complex **Mn6**

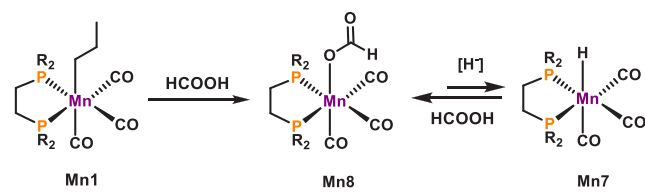
was observed in the $^{31}\text{P}\{^1\text{H}\}$ NMR monitoring (Figure 5b) as a singlet at 86.8 ppm, with a broad signal at 7.92 ppm in the corresponding ^1H NMR spectrum, at a chemical shift value expected for a Mn-formato species (Figure S18). Thus, in the absence of more conclusive evidence, we tentatively assign the structure of **Mn6** as *trans*-[Mn(κ -O-OCHO)(dippe)-(CO)₂(dmsO)]. Next, the transient species **Mn7**, observed at 115.2 ppm, was identified as the known complex *fac*-[MnH(dippe)(CO)₃] by comparison with literature data²² and independent synthesis in our laboratories (see the Supporting Information). **Mn8** was observed as a broad signal at 89.5 ppm in the $^{31}\text{P}\{^1\text{H}\}$ NMR monitoring (Figure 5c). It was independently obtained by treating **Mn1** with an excess of formic acid (see the Supporting Information). In the ^1H NMR spectrum (Figure S.24), a sharp signal at 8.17 ppm was observed, at a chemical shift value expected for Mn-OCHO moieties. Based on these data, we assign the formula *fac*-[Mn(κ -O-OCHO)(dippe)(CO)₃] to **Mn8**. The chemical drawings of complexes **Mn5**–**8** are shown in Chart 3.

Chart 3. Chemical Drawings of Complexes **Mn5**–**8**



Further tests showed that **Mn7** does not react with CO₂ (1 bar) even if heated to 60 °C for several days. On the other hand, in a separate test, the reaction of **Mn8** with HBpin (excess) produced an unknown boron compound and **Mn7** (Figure S.28). Based on these observations, we suggest that **Mn8** generates from the reaction of **Mn1** with HCOOH formed *in situ* at the beginning of the catalytic run.¹³ Next, the interaction of **Mn8** with a hydride source would give **Mn7**, as shown in Scheme 2. In the presence of even small quantities of HCOOH in solution, **Mn7** may revert to the more thermodynamically stable **Mn8**.

Scheme 2. Proposed Side Reactions Leading to **Mn8** and **Mn7** from **Mn1**



Similarly, **Mn6** may form upon reaction of **Mn5** with HCOOH. In fact, the addition of CO₂ (1 atm) to a NMR tube containing **Mn5** in dmsO-*d*₆ gave no reaction even after prolonged heating to 60 °C. The two Mn-formato complexes **Mn6** and **Mn8** thus represent resting states of the catalyst, as observed by $^{31}\text{P}\{^1\text{H}\}$ NMR monitoring at the end of the catalytic run (Figure 5e).

Catalyst-free reduction of organic acids to the corresponding alcohols using HBpin was recently reported to occur via facile deoxygenative hydroboration of carboxylic acids to boronate esters and following hydrolysis.²³ In the framework of the

present study, it was therefore important to establish whether the catalyst plays a role in further reduction of HCOOH. To assess this, a NMR tube was charged with dmsO-*d*₆, HCOOH (0.265 mmol), and HBpin at different stoichiometric ratios (1:1; 1:2; 1:5 to HCOOH) under nitrogen. After heating to 60 °C for 24 h, in all cases, only (OCHO)Bpin (**A**) was observed as product in the absence of catalyst. This experiment was then repeated using a HCOOH/HBpin = 1:1 ratio under otherwise identical conditions, adding **Mn1** (2.65 μmol), this time observing the formation of products **A** and **C** in 1:1 ratio (see the Supporting Information), thus confirming the role of the catalyst in the reduction steps beyond HCOOH. The corresponding $^{31}\text{P}\{^1\text{H}\}$ NMR spectrum (Figure S.33), measured at the end of the reaction, showed also for this set of experiments the signals at 89.5 and 86.8 ppm due to **Mn6** and **Mn8**, respectively, as expected upon formation of stable Mn-formato species as catalyst resting states.

CONCLUSIONS

In summary, we have demonstrated that selected Mn(I) complexes supported by simple, commercially available non-pincer-type ligands such as 1,2-bis(diisopropylphosphino)ethane (dippe) are able to bring about the selective hydroboration of CO₂ to methoxyborane, representing an example of CO₂ utilization as C1 building block for chemical synthesis, catalyzed by earth-abundant transition metals. Essentially, quantitative yields (>99.9%) in the desired product were obtained using as low as 1 mol % of catalysts under mild reaction conditions (1 bar CO₂, 25–60 °C) within 5 to 24 h, depending on the complex used, in the absence of any base or additive, representing a significant improvement over known protocols based on Mn.

EXPERIMENTAL SECTION

Typical Procedure for CO₂ Hydroboration (NMR Tube Scale). A stock solution containing the catalyst (0.56–2.24 × 10^{−3} mmol), HBpin (0.224 mmol), and mesitylene as internal standard (0.056 mmol) in the desired solvent (0.4 mL) was added under nitrogen to a J-Young NMR tube. Once prepared, the sample was degassed via three freeze–pump–thaw cycles and then CO₂ (1 bar) was added using a Schlenk line. The NMR tube was then placed in an oil bath kept at the desired temperature (25, 40, 60, 80, or 100 °C) for the set reaction time. The formation of C1-products was monitored throughout the duration of the experiment using ^1H NMR spectroscopy and quantified by signal integration versus the mesitylene internal standard. Additional $^{31}\text{P}\{^1\text{H}\}$ and ^{11}B NMR spectra were also run to obtain further qualitative information. Each test was repeated at least twice to check for reproducibility. The yields of C1-products were obtained with an average error of ca. 6%.

Typical Procedure for CO₂ Hydroboration (Schlenk Tube Scale). The procedure described above was adapted for a Schlenk tube scale test. **Mn1** (2.24 × 10^{−2} mmol) was dissolved in dmsO-*d*₆ (4.0 mL) in a Schlenk tube equipped with a Rotaflo Teflon cap. HBpin (2.24 mmol) and mesitylene as internal standard (0.56 mmol) were then added under nitrogen to the mixture. The solution was frozen using a liquid nitrogen bath; the tube was degassed via three freeze–pump–thaw cycles, and then, CO₂ (1 bar) was added using a Schlenk line. The tube was warmed to room temperature and then heated to 60 °C for 24 h. At the end of the reaction, the excess CO₂ was

vented and an aliquot of the solution was analyzed by ^1H NMR. $(\text{CH}_3\text{O})\text{Bpin}$ was obtained in >99.9% yield as determined by integration of the ^1H NMR signal at 3.48 ppm against the internal standard. The test was repeated twice to check for reproducibility.

Synthesis of *fac*- $[\text{Mn}(\text{CH}_2\text{CH}_2\text{CH}_3)(\text{dcpe})(\text{CO})_3]$ (**Mn2**).

This compound was prepared using the precursor $[\text{MnBr}(\text{dcpe})(\text{CO})_3]$ that was synthesized according to the literature.²⁴ **Mn2** was subsequently prepared in analogous fashion to **Mn1**¹⁶ using $[\text{MnBr}(\text{dcpe})(\text{CO})_3]$ (0.765 g, 1.27 mmol) and propyl bromide (17 mL). Crude **Mn2** was extracted with *n*-pentane (90 mL), and the solvent was removed in vacuo to yield a pale yellow solid (0.359 g, 47%). ^1H NMR (δ , 400 MHz, C_6D_6 , 20 °C): 2.29–1.88 (m, 14H), 1.85–1.04 (m, 39H), 0.36 (quin, $J = 8.5$ Hz, 2H). $^{13}\text{C}\{^1\text{H}\}$ NMR (δ , 101 MHz, C_6D_6 , 20 °C): 227.9 (CO), 220.5 (CO), 40.2 (vt, $J = 10.1$ Hz), 35.0 (vt, $J = 7.0$ Hz), 31.3 (vt, $J = 3.8$ Hz), 31.1, 30.8, 29.8, 29.2, 28.5–27.9 (m), 27.0, 26.7, 22.5 (vt, $J = 18.0$ Hz), 12.0 (vt, $J = 14.7$ Hz). $^{31}\text{P}\{^1\text{H}\}$ NMR (δ , 162 MHz, C_6D_6 , 20 °C): 82.9 (s). ATR-IR (solid, cm^{-1}): 1969 (ν_{CO}), 1895 (ν_{CO}), 1855 (ν_{CO}). HRMS (TOF ESI⁺): m/z calculated for $\text{C}_{32}\text{H}_{55}\text{MnO}_3\text{P}_2$ $[\text{M} - \text{H}]^+$: 605.3079, found 605.3098.

Synthesis of *cis*- $[\text{MnH}(\text{dippe})(\text{CO})_2(\kappa\text{-5-dmso})]$ (**Mn5**).

To a solution of **Mn1** (15 mg, 3.36×10^{-5} mmol) in THF (0.5 mL), pinacolborane (8.6 mg, 6.72×10^{-5} mmol, 2 equiv) and $\text{dms}\text{-}d_6$ (4.24 mg, 5.04×10^{-5} mmol, 1.5 equiv) were added. The solution was stirred at 60 °C for 4 h, monitoring by $^{31}\text{P}\{^1\text{H}\}$ NMR. All volatiles were then removed in vacuo. The obtained white solid was dried in vacuo and analyzed by ^1H and $^{31}\text{P}\{^1\text{H}\}$ NMR spectroscopy. The complex, highly soluble in most common organic solvents, was obtained with impurities derived from byproducts of pinacolborane redistribution. Yield (crude): 65%. ^1H NMR (δ , 400 MHz, $\text{dms}\text{-}d_6$, 20 °C): 2.5 (m), 2.23 (m), 2.03 (m), 1.78 (m), 1.63 (m), 1.37 (m), 1.21–1.05 (m), –6.90, –7.02 ppm (dd, $^2J_{\text{HP}} = 49.2$, $^2J_{\text{HP}} = 49.3$ Hz, 1H). $^{31}\text{P}\{^1\text{H}\}$ NMR (δ , 162 MHz, $\text{dms}\text{-}d_6$, 20 °C): 123.11 (d, $^2J_{\text{PP}} = 21.9$ Hz), 107.41 (d, $^2J_{\text{PP}} = 22.7$ Hz).

■ ASSOCIATED CONTENT

SI Supporting Information

The Supporting Information is available free of charge at <https://pubs.acs.org/doi/10.1021/acscatal.3c00020>.

General methods and materials, synthesis and characterization of manganese complexes, general procedures for catalytic tests, tables of catalytic data, additional NMR experiments, and selected NMR spectra (PDF)

■ AUTHOR INFORMATION

Corresponding Authors

Karl Kirchner – Institute of Applied Synthetic Chemistry, Vienna University of Technology, A-1060 Wien, Austria; Email: karl.kirchner@tuwien.ac.at

Luca Gonsalvi – Consiglio Nazionale delle Ricerche (CNR), Istituto di Chimica dei Composti Organometallici (ICCOM), 50019 Firenze, Italy; orcid.org/0000-0002-5996-6307; Email: l.gonsalvi@iccom.cnr.it

Authors

Sylwia Kostera – Consiglio Nazionale delle Ricerche (CNR), Istituto di Chimica dei Composti Organometallici (ICCOM), 50019 Firenze, Italy

Stefan Weber – Institute of Applied Synthetic Chemistry, Vienna University of Technology, A-1060 Wien, Austria
Ines Blaha – Institute of Applied Synthetic Chemistry, Vienna University of Technology, A-1060 Wien, Austria
Maurizio Peruzzini – Consiglio Nazionale delle Ricerche (CNR), Istituto di Chimica dei Composti Organometallici (ICCOM), 50019 Firenze, Italy

Complete contact information is available at: <https://pubs.acs.org/doi/10.1021/acscatal.3c00020>

Funding

Open Access is funded by the Austrian Science Fund (FWF).

Notes

The authors declare no competing financial interest.

■ ACKNOWLEDGMENTS

The MITE - ENEA - CNR Agreement Program within the National Recovery and Resilience Plan (PNRR) Mission 2 – Component 2 – Investment 3.5 “Research and Development on Hydrogen”, funded by The European Union – “Next Generation EU”, is gratefully acknowledged for financial support. CNR is also thanked for additional support through project ORCAS (project code DCM.AD004.063.001). K.K. gratefully acknowledges the financial support of the Austrian Science Fund (FWF) (Project No. P 33016-N).

■ REFERENCES

- (1) (a) Creel, E. B.; McCloskey, B. D. Scalable CO_2 -to-oxygenate production. *Nat. Catal.* **2018**, *1*, 6–7. (b) Voiry, D.; Shin, H.; Loh, K.; Chhowalla, M. Low-dimensional catalysts for hydrogen evolution and CO_2 reduction. *Nat. Rev. Chem.* **2018**, *2*, 0105. (c) Kattel, S.; Ramirez, P. J.; Chen, J. G.; Rodriguez, J. A.; Liu, P. Active sites for CO_2 hydrogenation to methanol on Cu/ZnO catalysts. *Science* **2017**, *355* (6331), 1296–1299. (d) Huang, K.; Sun, C. L.; Shi, Z. J. Transition-metal-catalyzed C–C bond formation through the fixation of carbon dioxide. *Chem. Soc. Rev.* **2011**, *40*, 2435–2452. (e) Schneider, J.; Jia, H.; Muckerman, J. T.; Fujita, E. Thermodynamics and kinetics of CO_2 , CO, and H^+ binding to the metal centre of CO_2 reduction catalysts. *Chem. Soc. Rev.* **2012**, *41*, 2036–2051. (f) Appel, A. M.; Bercaw, J. E.; Bocarsly, A. B.; Dobbek, H.; DuBois, D. L.; Dupuis, M.; Ferry, J. G. E.; Fujita, R.; Hille, P. J.; Kenis, A.; Kerfeld, C. A.; Morris, R. H.; Peden, C. H. F.; Portis, A. R.; Ragsdale, S. W.; Rauchfuss, T. B.; Reek, J. N. H.; Seefeldt, L. C.; Thauer, R. K.; Waldrop, G. L. Frontiers, Opportunities, and Challenges in Biochemical and Chemical Catalysis of CO_2 Fixation. *Chem. Rev.* **2013**, *113*, 6621–6658. (g) Cokoja, M.; Bruckmeier, C.; Rieger, B.; Herrmann, W. A.; Kühn, F. E. Transformation of Carbon Dioxide with Homogeneous Transition-Metal Catalysts: A Molecular Solution to a Global Challenge? *Angew. Chem., Int. Ed.* **2011**, *50*, 8510–8537. (h) Sakakura, T.; Choi, J.-C.; Yasuda, H. Transformation of Carbon Dioxide. *Chem. Rev.* **2007**, *107*, 2365–2387.
- (2) (a) Aresta, M., Ed. *Carbon Dioxide as Chemical Feedstock*; Wiley-VCH Verlag GmbH & Co. KGaA, 2010. (b) Peters, M.; Kohler, B.; Kuckshinrichs, W.; Leitner, W.; Markewitz, P.; Müller, T. E. Chemical Technologies for Exploiting and Recycling Carbon Dioxide into the Value Chain. *ChemSusChem* **2011**, *4*, 1216–1240. (c) Liu, Q.; Wu, L.; Jackstell, R.; Beller, M. Using carbon dioxide as a building block in organic synthesis. *Nat. Commun.* **2015**, *6*, 5933. (d) Klankermayer, J.; Wesselbaum, S.; Beydoun, K.; Leitner, W. Selective Catalytic Synthesis Using the Combination of Carbon Dioxide and Hydrogen: Catalytic Chess at the Interface of Energy and Chemistry. *Angew. Chem., Int. Ed.* **2016**, *55*, 7296–7343. (e) Artz, J.; Müller, T. E.; Thenert, K.; Kleinekorte, J.; Meys, R.; Sternberg, A.; Bardow, A.; Leitner, W. Sustainable Conversion of Carbon Dioxide: An Integrated Review of Catalysis and Life Cycle Assessment. *Chem. Rev.* **2018**, *118*, 434–504.

- (3) https://www.irena.org/-/media/Files/IRENA/Agency/Publication/2021/Jan/IRENA_Innovation_Renewable_Methanol_2021.pdf.
- (4) Dalena, F.; Senatore, A.; Marino, A.; Gordano, A.; Basile, M.; Basile, A. *Chapter 1 - Methanol Production and Applications: An Overview*; Basile, A., Dalena, F., Eds.; Elsevier, 2018; pp 3–28.
- (5) (a) Chakraborty, S.; Zhang, J.; Krause, J. A.; Guan, H. An Efficient Nickel Catalyst for the Reduction of Carbon Dioxide with a Borane. *J. Am. Chem. Soc.* **2010**, *132*, 8872–8873. (b) Chakraborty, S.; Patel, Y. J.; Krause, J. A.; Guan, H. Catalytic properties of nickel bis(phosphinite) pincer complexes in the reduction of CO₂ to methanol derivatives. *Polyhedron* **2012**, *32*, 30–34. (c) Chakraborty, S.; Zhang, J.; Patel, Y. J.; Krause, J. A.; Guan, H. Pincer-Ligated Nickel Hydridoborate Complexes: the Dormant Species in Catalytic Reduction of Carbon Dioxide with Boranes. *Inorg. Chem.* **2013**, *52*, 37–47. (d) Bertini, F.; Glatz, M.; Stöger, B.; Peruzzini, M.; Veiros, L. F.; Kirchner, K.; Gonsalvi, L. Carbon Dioxide Reduction to Methanol Catalyzed by Mn(I) PNP Pincer Complexes under Mild Reaction Conditions. *ACS Catal.* **2019**, *9*, 632–639. (e) Das Neves Gomes, C.; Blondiaux, E.; Thuéry, P.; Cantat, T. Metal-Free Reduction of CO₂ with Hydroboranes: Two Efficient Pathways at Play for the Reduction of CO₂ to Methanol. *Chem.—Eur. J.* **2014**, *20*, 7098–7106. (f) Lu, Z.; Williams, T. J. Di(carbene)-Supported Nickel Systems for CO₂ Reduction Under Ambient Conditions. *ACS Catal.* **2016**, *6*, 6670–6673.
- (6) (a) Bontemps, S.; Vendier, L.; Sabo-Etienne, S. Borane-Mediated Carbon Dioxide Reduction at Ruthenium: Formation of C1 and C2 Compounds. *Angew. Chem., Int. Ed.* **2012**, *51*, 1671–1674. (b) Ma, Q. Q.; Liu, T.; Li, S.; Zhang, J.; Chen, X.; Guan, H. Highly efficient reduction of carbon dioxide with a borane catalyzed by bis(phosphinite) pincer ligated palladium thiolate complexes. *Chem. Commun.* **2016**, *52*, 14262–14265. (c) Wesselbaum, S.; Moha, V.; Meuresch, M.; Brosinski, S.; Thenert, K. M.; Kothe, J.; vom Stein, T.; Englert, U.; Hölscher, M.; Klankermayer, J.; Leitner, W. Hydrogenation of carbon dioxide to methanol using a homogeneous ruthenium–Triphos catalyst: from mechanistic investigations to multiphase catalysis. *Chem. Sci.* **2015**, *6*, 693–704. (d) Rezaee, N. M.; Huff, C. A.; Sanford, M. S. Tandem Amine and Ruthenium-Catalyzed Hydrogenation of CO₂ to Methanol. *J. Am. Chem. Soc.* **2015**, *137*, 1028–1031. (e) Kothandaraman, J.; Goepfert, A.; Czaun, M.; Olah, G. A.; Surya Prakash, G. K. Conversion of CO₂ from Air into Methanol Using a Polyamine and a Homogeneous Ruthenium Catalyst. *J. Am. Chem. Soc.* **2016**, *138*, 778–781.
- (7) (a) Wang, T.; Stephan, D. W. Carbene-9-BBN Ring Expansions as a Route to Intramolecular Frustrated Lewis Pairs for CO₂ Reduction. *Chem.—Eur. J.* **2014**, *20*, 3036–3039. (b) Fontaine, F. G.; Courtemanche, M. A.; Légaré, M. A. Transition-Metal-Free Catalytic Reduction of Carbon Dioxide. *Chem.—Eur. J.* **2014**, *20*, 2990–2996. (c) Courtemanche, M. A.; Légaré, M. A.; Maron, L.; Fontaine, F. G. A Highly Active Phosphine–Borane Organocatalyst for the Reduction of CO₂ to Methanol Using Hydroboranes. *J. Am. Chem. Soc.* **2013**, *135*, 9326–9329. (d) Riduan, S. N.; Zhang, Y.; Ying, J. Y. Conversion of carbon dioxide into methanol with silanes over N-heterocyclic carbene catalysts. *Angew. Chem., Int. Ed.* **2009**, *48*, 3322–3325. (e) Ashley, A. E.; Thompson, A. L.; O'Hare, D. Non-Metal-Mediated Homogeneous Hydrogenation of CO₂ to CH₃OH. *Angew. Chem., Int. Ed.* **2009**, *48*, 9839–9843. (f) Ménard, G.; Stephan, D. W. Room Temperature Reduction of CO₂ to Methanol by Al-Based Frustrated Lewis Pairs and Ammonia Borane. *J. Am. Chem. Soc.* **2010**, *132*, 1796–1797.
- (8) Kostera, S.; Peruzzini, M.; Gonsalvi, L. Recent Advances in Metal Catalyst Design for CO₂ Hydroboration to C1 Derivatives. *Catalysts* **2021**, *11* (1), 58.
- (9) (a) Li, L.; Zhu, H.; Liu, L.; Song, D.; Lei, M. A Hydride-Shuttle Mechanism for the Catalytic Hydroboration of CO₂. *Inorg. Chem.* **2018**, *57*, 3054–3060. (b) Espinosa, M. R.; Charboneau, D. J.; de Oliveira, A. G.; Hazari, N. Controlling Selectivity in the Hydroboration of Carbon Dioxide to the Formic Acid, Formaldehyde, and Methanol Oxidation Levels. *ACS Catal.* **2019**, *9*, 301–314.
- (c) Sánchez, P.; Hernández-Juárez, M.; Rendón, N.; López-Serrano, J.; Álvarez, E.; Paneque, M.; Suárez, A. Hydroboration of carbon dioxide with catechol- and pinacolborane using an Ir–CNP* pincer complex. Water influence on the catalytic activity. *Dalton Trans.* **2018**, *47*, 16766–16776.
- (10) (a) Gonsalvi, L.; Guerriero, A.; Kostera, S. Chapter 3: Homogeneously Catalyzed CO₂ Hydrogenation to Formic Acid/Formate with Non-Precious Metal Catalysts. In *CO₂ Hydrogenation Catalysis*, 1st ed. March; Himeda, Y.; Ed.; Wiley-VCH: Weinheim, Germany; pp 53–88. (b) Holzwarth, M. S.; Plietker, B. Biorelevant Metals in Sustainable Metal Catalysis—A Survey. *ChemCatChem.* **2013**, *5*, 1650–1679. (c) Bertini, F.; Glatz, M.; Gorgas, N.; Stöger, B.; Peruzzini, M.; Veiros, L. F.; Kirchner, K.; Gonsalvi, L. Carbon Dioxide Hydrogenation Catalysed by Well-defined Mn(I) PNP Pincer Hydride Complexes. *Chem. Sci.* **2017**, *8*, 5024–5029. (d) Valyaev, D. A.; Lavigne, G.; Lugan, N. Manganese organometallic compounds in homogeneous catalysis: Past, present, and prospects. *Coord. Chem. Rev.* **2016**, *308* (2), 191–235. (e) Kallmeier, F.; Kempe, R. Manganese Complexes for (De)Hydrogenation Catalysis: A Comparison to Cobalt and Iron Catalysts. *Angew. Chem., Int. Ed.* **2018**, *57*, 46–60. (f) Yang, W.; Chernyshov, I. Y.; van Schendel, R. K. A.; Weber, M.; Müller, C.; Filonenko, G. A.; Pidko, E. A. Robust and efficient hydrogenation of carbonyl compounds catalysed by mixed donor Mn(I) pincer complexes. *Nat. Commun.* **2021**, *12*, 12.
- (11) Erken, C.; Kaithal, A.; Sen, S.; Weyhermüller, T.; Hölscher, M.; Werlé, C.; Leitner, W. Manganese-catalyzed hydroboration of carbon dioxide and other challenging carbonyl groups. *Nat. Commun.* **2018**, *9*, 4521.
- (12) (a) Wan, X.; Li, M.; Liao, R.-Z. Ligand-assisted Hydride Transfer: A Pivotal Step for CO₂ Hydroboration Catalyzed by a Mononuclear Mn(I) PNP Complex. *Chem. Asian J.* **2021**, *16*, 2529–2537. (b) Zhang, L.; Zhao, Y.; Liu, C.; Pu, M.; Lei, M.; Cao, Z. Hydroboration of CO₂ to Methyl Boronate Catalyzed by a Manganese Pincer Complex: Insights into the Reaction Mechanism and Ligand Effect. *Inorg. Chem.* **2022**, *61* (14), 5616–5625.
- (13) Kostera, S.; Peruzzini, M.; Kirchner, K.; Gonsalvi, L. Mild and Selective Carbon Dioxide Hydroboration to Methoxyboranes Catalyzed by Mn(I) PNP Pincer Complexes. *ChemCatChem.* **2020**, *12*, 4625–4631.
- (14) Ghosh, P.; Jacobi von Wangelin, A. Manganese-Catalyzed Hydroborations with Broad Scope. *Angew. Chem., Int. Ed.* **2021**, *60*, 16035–16043.
- (15) (a) Weber, S.; Kirchner, K. Manganese Alkyl Carbonyl Complexes: From Iconic Stoichiometric Textbook Reactions to Catalytic Applications. *Acc. Chem. Res.* **2022**, *55*, 2740–2751. (b) Garduño, J. A.; García, J. J. Toward Amines, Imines, and Imidazoles: A Viewpoint on the 3d Transition-Metal-Catalyzed Homogeneous Hydrogenation of Nitriles. *ACS Catal.* **2020**, *10*, 8012–8022.
- (16) Weber, S.; Stöger, B.; Veiros, L. F.; Kirchner, K. Rethinking Basic Concepts - Hydrogenation of Alkenes Catalyzed by Bench-Stable Alkyl Mn(I) Complexes. *ACS Catal.* **2019**, *9*, 9715–9720.
- (17) Weber, S.; Glavic, M.; Stöger, B.; Pittenauer, E.; Podewitz, M.; Veiros, L. F.; Kirchner, K. Manganese-Catalyzed Dehydrogenative Silylation of Alkenes Following two Parallel Inner-Sphere Pathways. *J. Am. Chem. Soc.* **2021**, *143*, 17825–17832.
- (18) Weber, S.; Zobernig, D.; Stöger, B.; Veiros, L. F.; Kirchner, K. Hydroboration of Terminal Alkenes and *trans*-1,2-Diboration of Terminal Alkynes Catalyzed by a Mn(I) Alkyl Complex. *Angew. Chem., Int. Ed.* **2021**, *60*, 24488–24492.
- (19) Kostera, S.; Weber, S.; Peruzzini, M.; Veiros, L. F.; Kirchner, K.; Gonsalvi, L. Carbon Dioxide Hydrogenation to Formate Catalyzed by a Bench-Stable, Non-Pincer-Type Mn(I) Alkylcarbonyl Complex. *Organometallics* **2021**, *40*, 1213–1220.
- (20) Kraihanzel, C. M.; Maples, P. K. Structures of Acyl- and Methylmanganese Carbonyl Complexes of Chelating Diphosphines. *J. Organomet. Chem.* **1969**, *20*, 269–272.

(21) Yang, W.; Filonenko, G. A.; Pidko, E. A. Performance of homogeneous catalysts viewed in dynamics. *Chem. Commun.* **2023**, *59*, 1757–1768.

(22) Garduño, J. A.; García, J. J. Non-Pincer Mn(I) Organometallics for the Selective Catalytic Hydrogenation of Nitriles to Primary Amines. *ACS Catal.* **2019**, *9*, 392–401.

(23) (a) Harinath, A.; Bhattacharjee, J.; Panda, T. K. Facile reduction of carboxylic acids to primary alcohols under catalyst-free and solvent-free conditions. *Chem. Commun.* **2019**, *55*, 1386–1389.

(b) Xu, X.; Yan, D.; Zhu, Z.; Kang, Z.; Yao, Y.; Shen, Q.; Xue, M. Catalyst-Free Approach for Hydroboration of Carboxylic Acids under Mild Conditions. *ACS Omega* **2019**, *4*, 6775–6783.

(24) Garduño, J. A.; Flores-Alamo, M.; García, J. J. Manganese-Catalyzed Transfer Hydrogenation of Nitriles with 2-Butanol as the Hydrogen Source. *ChemCatChem.* **2019**, *11*, 5330–5338.